ACS Catalysis

pubs.acs.org/acscatalysis
Research Article

Practical Synthesis of Chiral Ferrocenenylphosphino-Gold(I) Catalysts and NEST Analysis of the Enantioinduction

Pablo Mora, Imma Escofet, Maria Besora, Federica Cester Bonati, and Antonio M. Echavarren*

Cite This: ACS Catal. 2025, 15, 2342−2350
Read Online

ACCESS | Metrics & More | Article Recommendations | Supporting Information

ABSTRACT: The concise modular synthesis of a family of monodentate 1,2-disubstituted ferrocene ligands containing a diaryl phosphine and a 2-aryl indole is described. Their gold(I) complexes were applied to the enantioselective gold(I)-catalyzed formal [4 + 2] cycloaddition of 1,6-arylenynes, the enyne cyclization/nucleophile addition of N-tethered 1,6-enynes, and the methoxycyclization of 1,6-arylenynes with high levels of enantioselectivity in all cases. Crystallographic and computational studies highlighted the relevant role of noncovalent interactions within the ligand scaffold and between the ligand and substrate in the modes of enantioinduction in the cyclization of unsaturated substrates. Our recently developed open-source tool NEST was applied to analyze the chiral pockets of the catalysts, which in combination with RDKit allowed us to understand the enantioselectivity in these reactions, paving the way for a predictive-based approach toward the rational development of chiral ligands for enantioselective Au(I) catalysis.

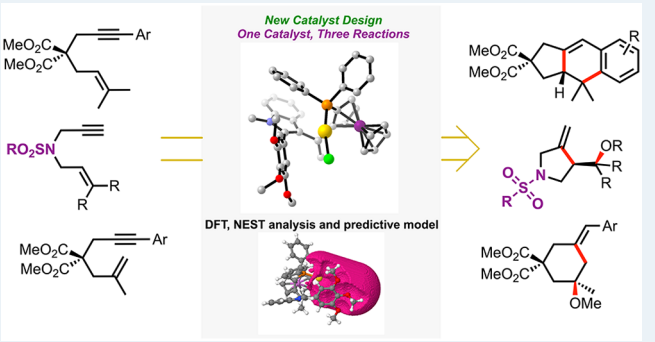

KEYWORDS: *gold catalysis, enynes, ferrocenyl ligand, cycloaddition, alkoxycyclization*

INTRODUCTION

The design of new chiral ligands plays an important role in the progress of asymmetric catalysis.[1] Ferrocenyl phosphines are arguably one of the most relevant and versatile classes of ligands for asymmetric metal-catalyzed transformations.[2] Since the pioneering work of Hayashi,[3] many other ligands based on ferrocene, such as Josiphos,[4] TaniaPhos,[5] Walphos,[6] Bophos,[7] Trifier,[8] and Zhaophos,[9] have been applied in a broad range of asymmetric metal-catalyzed transformations. Interestingly, the first example of enantioselective gold(I) catalysis relied on the use of a bifunctional gold(I) ferrocenyl phosphine catalyst in the asymmetric aldol-type reaction between aldehydes and isocyanoacetates.[10] Despite this pioneering work, the field of enantioselective gold(I) catalysis has been largely dominated by axially chiral binuclear gold(I) complexes[11−16] and monodentate phosphoramidite ligands.[17−20] Alternative strategies based on complexes with chiral counteranions[21−25] and/or hydrogen-bonding[26−29] have also been developed. Only recently, gold(I) ferrocene-based complexes have emerged as promising candidates for asymmetric gold(I) catalysis.[30−33]

Our group has reported the development of novel ligand designs tailored to meet the requirements imposed by the geometry of gold(I) (Figure 1).[30,32,34−37] Despite this considerable progress, ligand preparation is often lengthy[32,38] and, on occasion, chiral HPLC separation is required,[39,40] thus limiting expedient modifications of the catalyst structure.

Inspired by the work of Togni and Hu on heterocycle-containing ferrocenyl ligands,[41−44] we envisioned a new ligand scaffold based on a ferrocenyl phosphine containing an *N*-heterocycle. Here, we report the readily modular preparation of chiral gold(I) complexes with 1,2-disubstituted ferrocene ligands in only two steps from [1-(dimethylamino)ethyl]-2-(diphenylphosphino)ferrocene (PPFA), which is commercially available in either enantiomeric form, and their application in enantioselective gold(I) catalysis. This allowed us to test with this new catalyst design our recently developed open-source tool NEST,[36] based on DFT calculations and X-ray structural data, in combination with RDKit, to understand the enantioselectivity achieved in gold(I)-catalyzed cyclization reactions.

RESULTS AND DISCUSSION

A new library of gold(I) complexes has been built using a modular synthetic sequence based on 2-aryl indoles **3a−o** and commercially available (R,S_p)- or (S,R_p)-(PPFA) (**1**), which can also be easily obtained from Ugi's amine[45] (Scheme 1).

Received: December 4, 2024
Revised: January 8, 2025
Accepted: January 10, 2025
Published: January 24, 2025

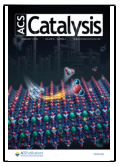

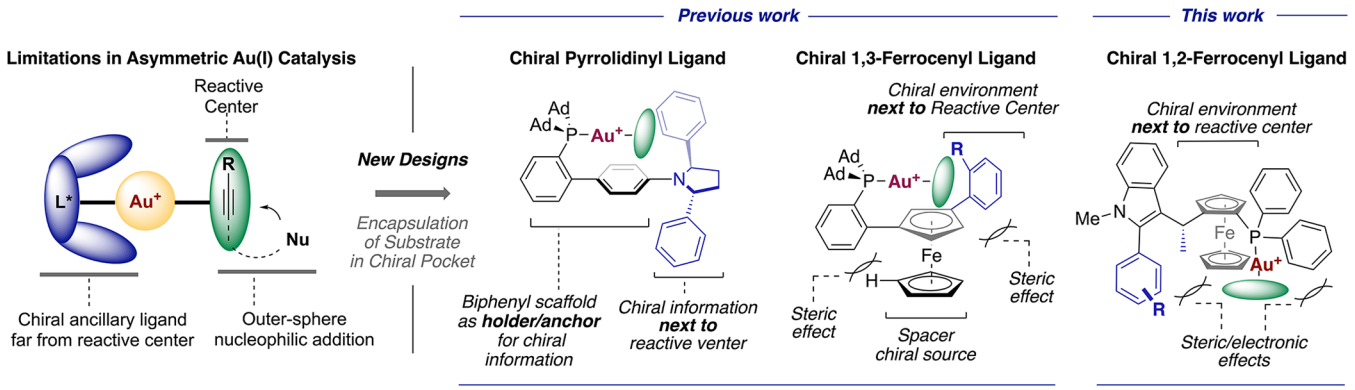

Figure 1. Design of chiral monodentate 1,2-ferrocene-based ligands for asymmetric gold(I) catalysis.

Scheme 1. Synthesis of Gold(I) Complexes A–Q from Ferrocenes 1 or 2[a]

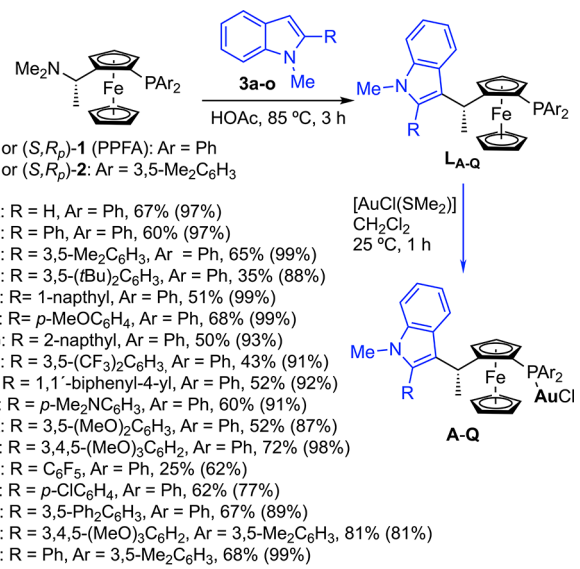

(*R*,*S*$_p$)-**1** or (*S*,*R*$_p$)-**1** (PPFA): Ar = Ph
(*R*,*S*$_p$)-**2** or (*S*,*R*$_p$)-**2**: Ar = 3,5-$Me_2C_6H_3$

(*R*,*R*$_p$)-**A**: R = H, Ar = Ph, 67% (97%)
(*R*,*R*$_p$)-**B**: R = Ph, Ar = Ph, 60% (97%)
(*R*,*R*$_p$)-**C**: R = 3,5-$Me_2C_6H_3$, Ar = Ph, 65% (99%)
(*R*,*R*$_p$)-**D**: R = 3,5-(*t*Bu)$_2C_6H_3$, Ar = Ph, 35% (88%)
(*R*,*R*$_p$)-**E**: R= 1-napthyl, Ar = Ph, 51% (99%)
(*R*,*R*$_p$)-**F**: R= *p*-$MeOC_6H_4$, Ar = Ph, 68% (99%)
(*R*,*R*$_p$)-**G**: R = 2-napthyl, Ar = Ph, 50% (93%)
(*R*,*R*$_p$)-**H**: R = 3,5-$(CF_3)_2C_6H_3$, Ar = Ph, 43% (91%)
(*R*,*R*$_p$)-**I**: R = 1,1′-biphenyl-4-yl, Ar = Ph, 52% (92%)
(*R*,*R*$_p$)-**J**: R = *p*-$Me_2NC_6H_3$, Ar = Ph, 60% (91%)
(*R*,*R*$_p$)-**K**: R = 3,5-$(MeO)_2C_6H_3$, Ar = Ph, 52% (87%)
(*R*,*R*$_p$)-**L**: R = 3,4,5-$(MeO)_3C_6H_2$, Ar = Ph, 72% (98%)
(*S*,*S*$_p$)-**M**: R = C_6F_5, Ar = Ph, 25% (62%)
(*S*,*S*$_p$)-**N**: R = *p*-ClC_6H_4, Ar = Ph, 62% (77%)
(*S*,*S*$_p$)-**O**: R = 3,5-$Ph_2C_6H_3$, Ar = Ph, 67% (89%)
(*R*,*R*$_p$)-**P**: R = 3,4,5-$(MeO)_3C_6H_2$, Ar = 3,5-$Me_2C_6H_3$, 81% (81%)
(*S*,*S*$_p$)-**Q**: R = Ph, Ar = 3,5-$Me_2C_6H_3$, 68% (99%)

[a]Yields for the complexation with ([AuCl(SMe_2)] in parentheses.

The reaction of PPFA with 2-substituted *N*-methylindoles afforded the chiral ligands $\mathbf{L_{A-O}}$, which upon complexation with [AuCl(SMe2)] led to complexes **A**–**O** in moderate to good yields, with the exception of **D**, **H**, and **M** in which the corresponding ligands bearing very bulky or electron-withdrawing R groups were obtained in 25–43% yields. Complexes **P** and **Q** were similarly prepared from **2** (Ar = 3,5-$Me_2C_6H_3$). The structures of complexes **A**–**B**, **G**–**H**, **L**, and **P** were confirmed by X-ray diffraction (Figure 2).

We first prepared catalyst (*R*,*R*$_p$)-**A** derived from *N*-methylindole (**3a**) (Scheme 1) and examined its activity in the formal [4 + 2] intramolecular cycloaddition of 1,6-enyne **4a** to yield cycloadduct **5a**[46,47] (Table 1), a reaction that we have used to benchmark the performance of chiral gold(I) catalysts.[24,26,32,34,36] Although gold(I) complex **A** was active in the reaction, the cycloadduct was obtained in a nearly racemic form (Table 1, entry 1). Examination of the X-ray structure of (*R*,*R*$_p$)-**A** suggested that the lack of enantioinduction could be ascribed to insufficient shielding of the metal center by the 2-methylindole group (Figure 2). Therefore, a phenyl group at the *C*-2 position of the indole was introduced, leading to a new gold(I) complex (*R*,*R*$_p$)-**B**, whose performance resulted in a significant increase in enantioselectivity from 52:48 to 82:18 *er* (Table 1, entries 1–2).

Analysis of the crystallographic structure of complex (*R*,*R*$_p$)-**B** confirmed that the introduction of the pseudobiaryl fragment in the ligand blocks one side of the scaffold, creating a better defined chiral pocket (Figure 2). In the solid state, shorter distances were observed between the aryl ring at C-3 of the indole and the gold atom in complex **L** (3.413 Å) than in **B** (3.824 Å), **G** (3.714 Å), and **H** (3.657 Å). The X-ray crystal structure of the cationic complex (*R*,*R*$_p$)-$\mathbf{L_L}$Au(MeCN)NTf_2, prepared by the reaction of (*R*,*R*$_p$)-**L** with $AgNTf_2$ in CH_2Cl_2 in the presence of MeCN, revealed a reduction in the dihedral angle in the indole–aryl axis from 74.2° to 42.6° with respect to neutral (*R*,*R*$_p$)-**L**. The distance centroid-Au in the cationic complex is 3.59 Å, much shorter than that in the neutral complex (4.16 Å). This crystallographic information suggests the presence of weak Au–arene interactions, which are also present in other gold(I) complexes.[34,48−50] The torsion angle in the indole–aryl axis was significantly larger for complex **L** (−74.2°) than for the rest of this family of complexes.[51]

The introduction of two methyl groups at the 3,5-position of the aryl at C-2 of the indole in complex **C** led to a modest improvement in the enantioselectivity (Table 1, entry 3). However, increasing the steric bulk with two *tert*-butyl groups in **D** proved to be detrimental (Table 1, entry 4). Results with **E** and **F** (Table 1, entries 5 and 6) were very similar to those obtained with **B**. The presence of a 2-naphthyl group in **G** or a 3,5-$(CF_3)_2C_6H_3$ aryl in **H** led to **5a** in moderate yields and enantioselectivities (Table 1, entries 7 and 8). Product **5a** was obtained in poor yield and moderate enantioselectivity, with complex **I** bearing a biphenyl fragment at C-2 of the indole (Table 1, entry 9). On the other hand, whereas the presence of a *p*-Me_2N in **J** resulted in nearly racemic **5a** (Table 1, entry 10), complexes **K** and **L** with 3,5-dimethoxyphenyl or 3,4,5-trimethoxyphenyl rings, respectively, yielded **5a** in good yields and enantioselectivities (Table 1, entries 11 and 12). Cationic complex (*R*,*R*$_p$)-LAu(MeCN)NTf_2 exhibited a performance similar to that of **L**.[51]

Catalyst **M** with a C_6F_5 group at the C-2 of the indole led to lower enantioselectivity than **B** with a Ph group, whereas a *p*-ClC_6H_5 in **N** gave the same enantioselectivity (Table 1, compare entry 2 with entries 13 and 14). Replacement of the *tert*-butyl groups in **D** by Ph groups in **O** led to a decrease in the yield of **5a**, but with an improved enantiomeric excess (Table 1, entries 4 and 15). Finally, we found that changing the phenyl groups at the phosphine to 3,5-$Me_2C_6H_3$ groups in

https://doi.org/10.1021/acscatal.4c07495
ACS Catal. 2025, 15, 2342−2350

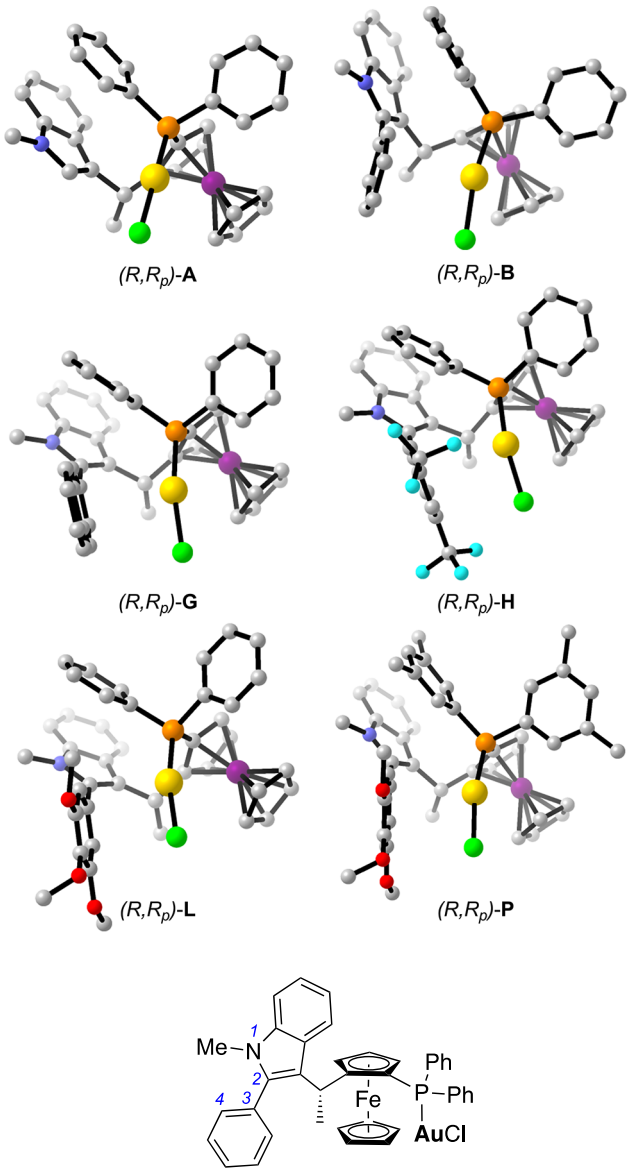

	A	B	G	H	L	P
d(Au-C$_3$)	4.152	3.824	3.714	3.657	3.413	3.434
^(1-2-3-4)	-	-52.55	-55.26	-68.8	-74.2	-49.8

Figure 2. Selected X-ray crystal structures of complexes **A**, **B**, **G**, **H**, **L**, and **P**. Distances are expressed in Å and angles in degrees. Hydrogen atoms are omitted for clarity.

P and **Q** had a minor effect on the enantioselectivity (Table 1, compare entry 12 with entry 16 and entry 2 with entry 17).

The scope of the formal [4 + 2] cycloaddition of aryl 1,6-enynes **4a−m** was then explored using (R,R_p)-**L** (5 mol %) and $AgNTf_2$ (5 mol %) in CH_2Cl_2 at 25 °C (Scheme 2). Good to excellent enantioselectivities were obtained for **5a−e** (Scheme 2). Cyclization of **4f−g** bearing *o*-substituents at the aryl led to tricyclic adducts **5f−g** in good yields, although the enantioselectivity decreased slightly in the case of **5g**. Good to excellent yields and enantioselectivities were also obtained in the cyclization of substrates **4h−m** with different aryl or heteroaryl groups, alkene substitutions, or substituents at the 1,6-enyne tether.

Table 1. [4 + 2] Cycloaddition of Enyne 4a with Gold(I) Complexes A−Q

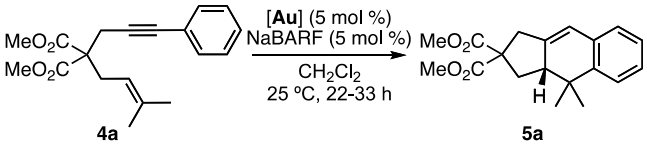

entry	Au catalyst	yield (%)[a]	er[b]
1	(R,R_p)-**A**	53	52:48
2	(R,R_p)-**B**	68	82:18
3	(R,R_p)-**C**	63	85:15
4	(R,R_p)-**D**	40	63:37
5	(R,R_p)-**E**	63	86:14
6	(R,R_p)-**F**	46	87:13
7	(R,R_p)-**G**	53	79:21
8	(R,R_p)-**H**	42	72:28
9	(R,R_p)-**I**	13	78:22
10	(R,R_p)-**J**	48	55:45
11	(R,R_p)-**K**	79	91.5:8.5
12	(R,R_p)-**L**	83	95.5:4.5
13	(S,S_p)-**M**	74	37:63
14	(S,S_p)-**N**	77	18:82
15	(S,S_p)-**O**	22	13.5:86.5
16	(R,R_p)-**P**	60	92:8
17	(S,S_p)-**Q**	75	20:80

[a]Determined by ^{1}H NMR against internal standard. [b]Determined by SFC on the chiral stationary phase.

Scheme 2. Enantioselective [4 + 2] Cycloaddition of Aryl-Substituted 1,6-Enynes 4a−m Catalyzed by (R,R_p)-L

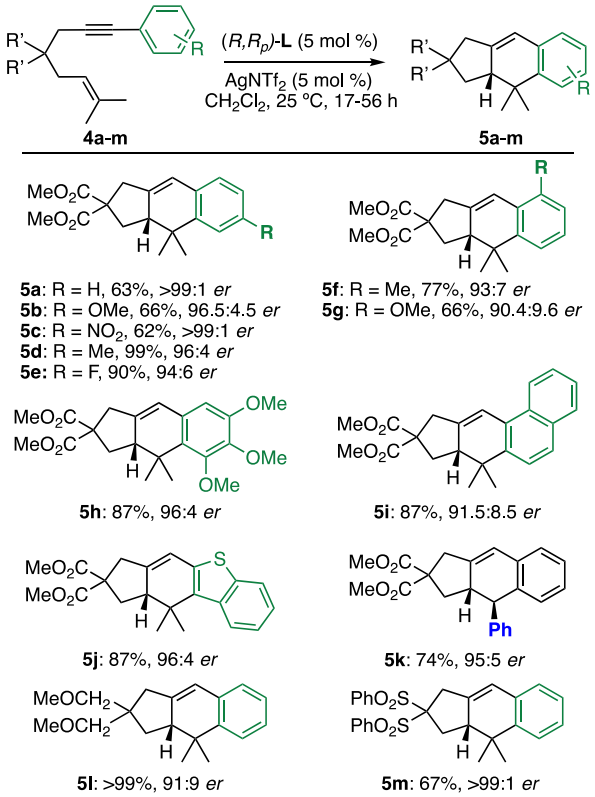

Complexes (R,R_p)-**L**, (S,S_p)-**L**, or (S,S_p)-$\mathbf{L}_L$Au(MeCN)NTf_2 were also found to be optimal[51] for the cyclization/nucleophile addition of *N*-tethered 1,6-enynes **6**, providing chiral

https://doi.org/10.1021/acscatal.4c07495
ACS Catal. 2025, 15, 2342−2350

pyrrolidines in good yields and high enantioselectivities (Scheme 3). Thus, alkoxycyclization products **7a−v** were obtained in good yields and good to excellent enantioselectivities from 1,6-enynes **6a−q** and alcohols. As expected,[26,52,53] diastereomeric products **7s** and **7t** were obtained from (*E*)- and (*Z*)-configured starting materials, respectively. The reaction was also extended to electron-rich C-nucleophiles such as indole and 1,3,5-trimethoxybenzene to provide enantiopure compounds **7w** and **7x**. In general, slightly better enantiomeric excesses were obtained with the more reactive (S,S_p)-$\mathbf{L}_\mathbf{L}$Au(MeCN)NTf_2, which also allowed us to lower the catalyst loading from 5 to 2.5 mol %.

Alkoxycyclization products **7d** and **7t** were readily converted into bicyclic products **8a** and **8b**, respectively, by ring-closing metathesis (Scheme 4).

Scheme 3. Enantioselective Cyclization/Nucleophile Addition of *N*-Tethered 1,6-Enynes 6a−q

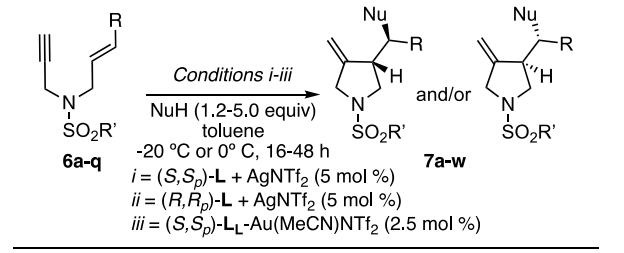

7a: R = Me, 80%, 98.5:1.5 *er (ii)*
7b: R = Et, 89%, 96:4 *er* (*ii*); 91%, 2:98 *er (i)*
7c: R = *i*Pr, 93%, 98:5:1.5 *er (ii)*
7d: R = Allyl, 86%, 97.5:2.5 *er (ii)*
7e: R = Bn, 98% 98:2 *er (ii)*

7f: R = *t*Bu, 62%, 92:8 *er (i)*; 77%, 97:3 *er* (*iii*)
7g: R = F, 78%, 97.5:2.5 *er* (*i*); 70%, >99:1 *er (iii)*
7h: R = Cl, 99%, >99:1 *er (i)*
7i: R = MeO, 99%, 97:3 *er* (*i*)
7j: R = NO_2, 60%, 97.5: 2.5 *er (i,* 0°C*)*; 60%, 96:4 *er (iii)*

7k: R = F, 72%, 94.5:5.5 *er (i)*; 67%, 94.5:5.5 *er (iii)*
7l: R = MeO, 83%, 97:3 *er (i)*; 83%, 98:2 *er (iii)*

7m: R = MeO, 90%, 98:2 *er (i)*
7n: R = NO_2, 95%, 92.5:7.5 *er (i,* 0°C*)*; 57%, >99:1 *er (iii)*

7o: 93%, 94:6 *er (i)*; 92%, >99:1 *er (iii)*

7p: 91%, >99:1 *er (i)*

7q: 50%, 95.5:4.5 *er (i)*; 72%, 98.5:1.5 *er (iii)*

7r: 99%, 97.5:2.5 *er (i)*

7s: 50%, 94:6 *er (i)*; 75%, >99:1 *er* (*iii*)

7t: 90%, 96.5:3.5 *er (i)*; 90%, >99:1 *er (iii)*

7u: R'= *p*-$O_2NC_6H_4$, 99% 98.5:1.5 *er (i)*

7v: R' = Me, 99%, >99:1 *er (i)* **7w**: 82%,[a] >99:1 *er (i)* **7x**: 81%, >99:1 *er (i)*

[a]3:1 ratio together with the product of indole attack at the carbene of the intermediate cyclopropyl gold(I) carbene.[51]

Scheme 4. Ring-Closing Metathesis of 7d and 7t

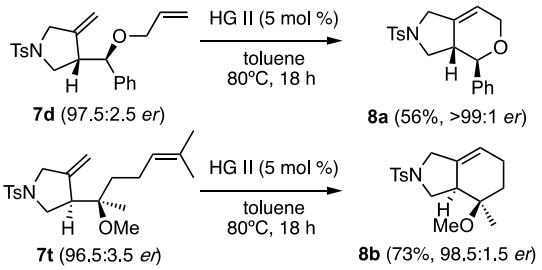

Similarly, the methoxycyclization of malonate-tethered aryl-substituted 1,6-aryl enynes **9a−i** yielded 1-methoxy-1-methyl-3-methylenecyclohexanes **10a−i** in good to excellent yields and enantioselectivities, which ranged from 85:15 to 93.5:6.5 *er* (Scheme 5). The absolute configuration of the resulting products was confirmed by X-ray diffraction of tosyl hydrazone **11**, obtained from **10c**.

Scheme 5. Enantioselective Methoxycyclization of Aryl-Substituted 1,6-Enynes 9a−i

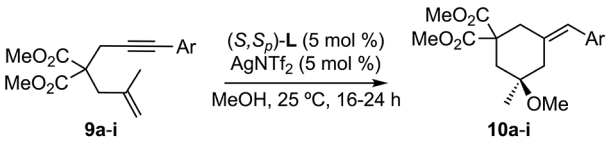

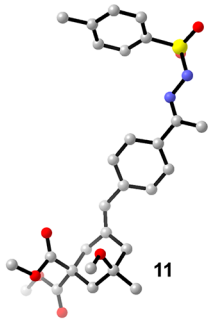

10a: Ar = Ph, 62%, 90.5:9.5 *er*
10b: Ar = *p*-$NO_2C_6H_4$, 68%, 86:14 *er*
10c: Ar = *p*-$MeCOC_6H_4$, 65%, 90:10 *er*
10d: Ar = *p*-FC_6H_4, 71%, 92:8 *er*
10e: Ar = *p*-$CF_3C_6H_4$, 57%, 91:9 *er*
10f: Ar = *o*-$MeOC_6H_4$, 86%, 93.5:6.5 *er*
10g: Ar = 2-napthyl, 95%, 85.5:14.5 *er*
10h: Ar = 3,5-$Me_2C_6H_3$, 95%, 90.5:9.5 *er*
10i: Ar = 2,3-$Cl_2C_6H_3$, 66%, 85:15 *er*

MECHANISTIC INVESTIGATIONS

To unveil the mode of enantioinduction of these novel ferrocenyl-based phosphine gold(I) complexes, we performed DFT calculations. BP86-D3/6-31G(d) (C, H, P, N, O, S) and SDD (Au, Fe) PCM = CH_2Cl_2 levels of theory were chosen due to their efficiency proved in our recent benchmark of DFT functionals using similar systems (Scheme 6).[54,55] We started our investigations by computing the reaction coordinate for the alkoxycyclization of substrate **6a** (Scheme 6a) with complex (R,R_p)-**L**. We calculated two possible minima resulting from the substrate coordinated to gold(I) through the alkyne [LAu(h^2-alkyne)]$^+$ (**Int1a-b**) and the reaction of the two enantiotopic *Re* and *Si* faces of the alkene (*R* and *S* pathways)

https://doi.org/10.1021/acscatal.4c07495
ACS Catal. 2025, 15, 2342−2350

Scheme 6. Schematic Representation of the Lowest-Energy Intermediates and Molecular Structures and NCI Plots of the Transition States[a] for the (a) Alkoxycyclization of *N*-Tethered 1,6-Enyne 6a and (b) [4 + 2] Cycloaddition of Aryl 1,6-Enyne 4a with Catalyst (R,R_p)-L

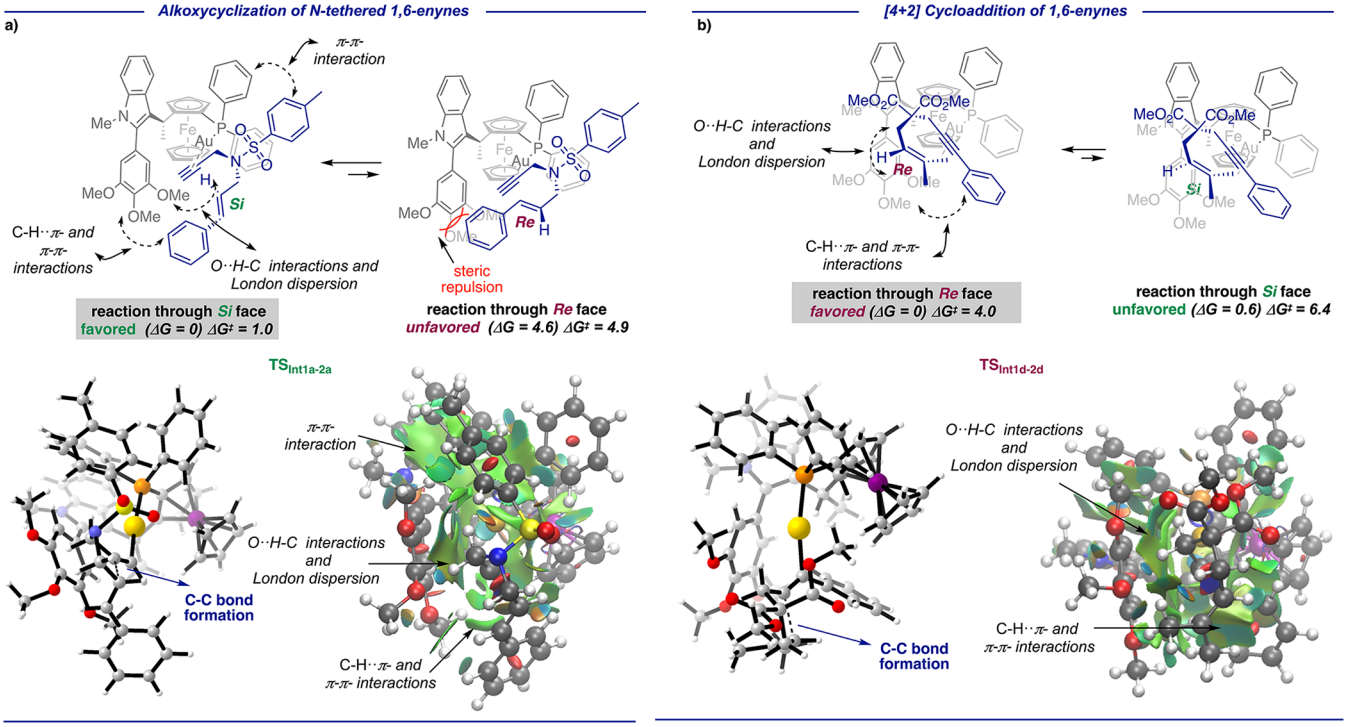

[a](S) pathways are depicted in green and (R) pathways in purple. CYLview representations and NCI plots of the two possible transition states $\mathbf{TS}_{\mathbf{Int1a-2a}}$ and $\mathbf{TS}_{\mathbf{Int1d-2d}}$ are displayed. Hydrogens are omitted for clarity. Color-filled RDG isosurface: strong attractive interactions are indicated in blue (C−C or C−N bond formation), weak attractive interactions are shown in green (noncovalent interactions), and strong repulsive interactions are shown in red. Color code: P, orange; Au, yellow; N, blue; O, red; C, gray; Fe, purple; and H, white. Energy values are given in kcal/mol relative to **Int1a** and **Int1d**, respectively.

in the intramolecular electrophilic addition as the enantiodetermining step of the transformation. We examined the evolution of the two possible gold(I) complexes **Int1a-b** following an exocyclic pathway, with **Int1a** being the most stable intermediate and the activation energy to reach $\mathbf{TS}_{\mathbf{Int1a-2a}}$ being lower than that of the other possible pathway ($\mathbf{TS}_{\mathbf{Int1b-2b}}$) by at least $\Delta G^{\ddagger}_{R\text{-}S}$ = 3.9 kcal/mol. Therefore, in agreement with the experimental results obtained with catalyst **L** (98.5:1.5 *er*) (Scheme 3), cyclopropyl gold(I) carbene **Int2a**, which leads to product **7a** with an *S* absolute configuration at C-3 of the pyrrolidine, is preferentially formed through the *Si* face of the alkene. As revealed by NCI plots,[56] attractive noncovalent interactions[57] between the aryl ring of the phosphine and the aryl ring of the tosyl moiety in the substrate and C−H−π[58] and London dispersion[59] interactions between the trimethoxy-substituted aryl ring of the indole and the aryl ring of the substrate play a major role in the chiral folding of the substrate and in the stabilization of the transition state ($\mathbf{TS}_{\mathbf{Int1a-2a}}$).

In the [4 + 2] cycloaddition of 1,6-enyne **4a** with the catalyst (R,R_p)-**L**, the reaction proceeds from the most stable [LAu(h^2-alkyne)]$^+$ intermediate **Int1d** through the lowest-energy transition state $\mathbf{TS}_{\mathbf{Int1d-2d}}$ (favored by 2.4 kcal/mol compared to the *S* pathway, $\mathbf{TS}_{\mathbf{Int1c-2c}}$) to yield product **5a** with *R* configuration, by the reaction of the alkyne through the *Re* prochiral face of the alkene (Scheme 6b). Attractive CH−π and π−π interactions between the aryl ring of the enyne and the trimethoxy-substituted aryl ring of the ligand are also stereocontrolling elements.

DATA ANALYSIS

The above presented experimental data on the enantiomerical ratio (*er*) for the [4 + 2] cycloaddition of enyne **4a** (Table 1) and the methoxycyclization of *N*-tethered 1,6-enyne **6a** (Tables S9 and S10 in the Supporting Information) for catalysts **B**−**I** and **K**−**Q** have been analyzed by constructing (multi)linear regression models with one or two chemical descriptors. This data analysis has a double aim: on the one hand, the elucidation of the determinant factors for enantioselectivity and on the other the evaluation of the prediction ability of the current approach as well as the performance of our recently developed descriptor NEST (see below). The present methodological strategy is similar to the one we used in previous studies.[36,60] The *er* data have been regressed in front of a total of 311 standardized descriptors: (i) derived from NEST,[36] a web tool designed on purpose by some of us for the description of quadrant volume occupation of catalysts bearing elongated ligands (Figure 3); (ii) obtained from DFT-optimized precatalyst (L−Au−Cl) structures, such as geometrical parameters or charges; (iii) based on the structure, such as Hammett parameters; (iv) automatically obtained from RDKit[61] (for a full list of descriptors, see Table S12 in the Supporting Information). The data analysis was carried out while results of *er* for catalysts **A**−**N** were available but not those for catalyst **O**−**Q**; hence, these were used to test

https://doi.org/10.1021/acscatal.4c07495
ACS Catal. 2025, 15, 2342−2350

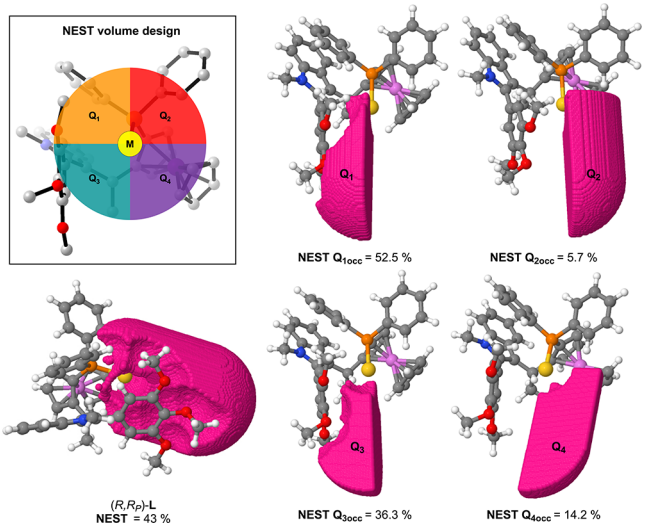

Figure 3. NEST volume design and an example of the NEST occupied volume of complex **L** (a = 5 Å).

the validity and the scope of the model. Catalyst **A** was left out of the analysis due structural differences from the rest of catalysts (lack of phenyl group at the *C-2* position of indole) (Figure 1), and **J** was excluded due to the lack of reactivity for methoxycyclization.[51]

In the data analysis of the *er* obtained for each catalyst in the [4 + 2] cycloaddition of enyne **4a**, we observed that a single descriptor was not enough to reproduce the *er*, due to low coefficients of determination (r^2 ≤0.45) and high mean squared error (MSE ≥ 5) and maximum absolute error (MAE ≥ 13) for the training set.[51] When two descriptors were used instead, the prediction ability was reached with several pairs of descriptors; with r^2 up to 0.89 and MAE down to 5.7 *er* for the training set, all pairs of descriptors with the best statistical results were carefully analyzed, also taking into account their chemical interpretability.[51] From this analysis, we selected the pair "NEST Min. horizontal 5" (descriptor 164) and "H bond and C−H π bond acceptor" (descriptor 226), which has r^2 = 0.86, MSE = 3.1, and MAE = 6.4 *er* for the training set. The combination of these two descriptors explained the experimental *er* and, at the same time, revealed the origin of the enantioselectivity. The "NEST Min. horizontal 5" is a steric measure of the space available in the catalyst; more precisely, it is the NEST[36] minimum horizontal occupation, the lowest value for the addition of the occupation of the two top quadrants (Q1 + Q2) or bottom (Q3 + Q4), with the phosphine oriented with the ferrocene carbon on the z axis and a NEST length of 5.

The descriptor "H bond and C−H π bond acceptor" measures the ability of the substituents on the phenyl ring at the *C2* position of the indole to set stabilizing interactions with the substrate by either accepting hydrogen bonds or C−H π interactions. This pair of descriptors applied to catalysts **O**−**Q** (test set) led to a very good agreement with an MAE of 6.5 *er*. The results are summarized in Table 2. Considering that catalysts in the test set (**O**−**Q**) present important structural changes with respect to the ones in the data set (**A**−**N**), the quality of the predictions is remarkable. These results support the idea that the pocket for the substrate in the catalyst and the ability to accept hydrogen bonds or C−H π interactions of the ligand govern the enantioselectivity.

Table 2. Results of Statistical Analysis

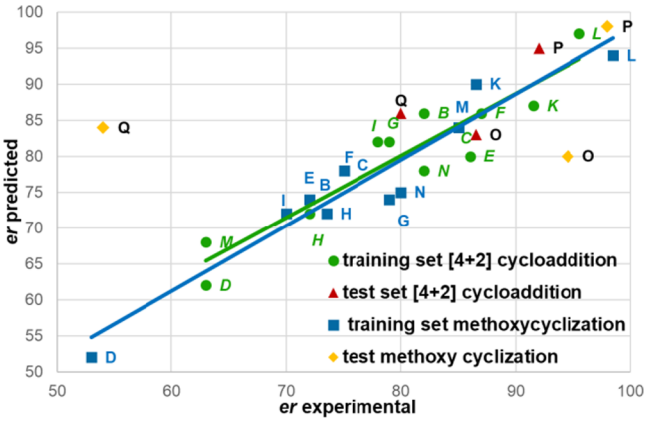

cat.	er [4 + 2][a] exp.[b]	er [4 + 2][a] pred.[b]	er methox.[c] exp.[b]	er methox.[c] pred.[b]
B	82:18	86:14	72:28	74:26
C	85:15	84:26	75:25	78:22
D	63:27	62:28	53:47	52:48
E	86:14	80:20	72:28	74:26
F	87:13	86:14	75:25	78:22
G	79:21	82:18	79:21	74:26
H	72:28	72:28	73.5	72:28
I	78:22	82:18	70:30	72:28
K	91.5:8.5	87:13	86.5:13.5	90:10
L	95.5:4.5	97:3	98.5:1.5	94:6
M	63:37[d]	68:32	85:15	84:16
N	82:18[d]	78:22	80:20	75:25
O	86.5:13.5[d]	83:27	94.5:5.5	80:20[e]
P	92:8	95:5	98:2	98:2
Q	80:20[d]	86:14	54:46	84:16

[a][4 + 2] Cycloaddition of enyne **4a**. [b]Exp. indicates experimental values (measurements); pred. indicates predicted values within the statistical model. [c]Methoxycyclization of enyne **6a**. [d]*er* for the opposite catalyst enantiomer (see Data Treatment in the Supporting Information). [e]Taking not the lowest-energy conformer of the precatalyst.

We then performed the analysis for the *er* obtained in the methoxycyclization of *N*-tethered 1,6-enyne **6a** (Scheme 3).[51] We found that, using one descriptor, the ability of the model to explain the results was slightly better than for the [4 + 2] cycloaddition of **4a** but still exhibited low r^2 ≤ 0.76, MSE ≥ 4, and MAE ≥ 14 for the training set.[51] When two descriptors were used, results improved up to r^2 ≤ 0.92, MSE ≥ 2.5, and MAE ≥ 4.3 for the training set. All best pairs of descriptors were carefully analyzed and the pair of descriptors "NEST Min. vertical 5" (descriptor 161) and "H bond and C−H π bond acceptor" (descriptor 226) was selected, with r^2 = 0.91, MSE = 2.8, and MAE = 5.0 *er* for the training set (see Table 2 and the Supporting Information for further details). The NEST minimum vertical occupation is the lowest value for the addition of the occupation of the two right quadrants (Q2 + Q4) or left (Q1 + Q3), with the same phosphine orientation and NEST length as for the [4 + 2] cycloaddition.[51] Note that the selected pair in this case is similar to the one for the [4 + 2] cycloaddition: the same descriptor for the ability of accepting hydrogen and C−H-π interactions and a similar NEST descriptor with different orientations of the two consecutive quadrants, horizontal in one and vertical in the other. This indicates that enyne **4a** and *N*-tethered 1,6-enyne **6a**

https://doi.org/10.1021/acscatal.4c07495
ACS Catal. 2025, 15, 2342−2350

coordinate in slightly different ways, and steric effects appear in different regions of the catalyst structure. When the test set was applied to this reaction, results were very good for catalyst **P** (98:2 *er* exp vs 98:2 *er* pred) but poor for catalysts **O** (94.5:5.5 *er* exp vs 70:30 *er* pred) and **Q** (54:46 *er* exp vs 84:16 *er* pred). For **O**, we suggest that the lowest-energy geometry of the catalyst is likely not the reactive one, as the large phenyl substituents block the coordination of the substrate. These phenyl groups can easily rotate and accommodate to a conformation with a slightly higher energy (1.3 kcal mol^{-1}); using this conformer, the prediction improved (94.5:5.5 *er* exp vs 80:20 *er* pred). For catalyst **Q**, we cannot quantitatively reproduce the observed enantioselectivity, but, considering that the enantiomeric ratio was low (similar to **A**) and knowing the bulkiness of the *N*-tosyl group, the reactive species for catalyst **Q** might need to undergo significant conformational changes for the coordination of enyne **6a**. Note that this does not occur in the [4 + 2] cycloaddition of **4a**, where the same catalysts are able to induce enantioselectivity.

CONCLUSIONS

In conclusion, we designed a new family of chiral gold(I) ferrocenyl phosphine complexes and applied them to the gold(I)-catalyzed enantioselective cyclization of three structurally different 1,6-enynes with excellent enantioselectivities. Noncovalent interactions were found to be key elements in the efficient folding of enynes by a combination of experimental, crystallographic, and computational methods. NEST analysis was applied to our system, which allowed for the validation and reliable prediction of enantioselectivities, highlighting the importance of the size and position of the free space for substrate coordination and the importance of attractive weak interactions. This work provides a platform for predicting and advancing rational ligand design for asymmetric gold(I) catalysis while streamlining the design of novel chiral ligand scaffolds.

ASSOCIATED CONTENT

Supporting Information

The Supporting Information is available free of charge at https://pubs.acs.org/doi/10.1021/acscatal.4c07495.

Experimental procedures, characterization data, NMR spectra, SFC and HPLC trace chromatograms, computational details, NEST analysis results, DFT calculations, and crystallographic data (PDF)

Accession Codes

CCDC 2406055−2406061 and 2406222 contain the supplementary crystallographic data for this paper. These data can be obtained free of charge via www.ccdc.cam.ac.uk/data_request/cif, or by emailing data_request@ccdc.cam.ac.uk, or by contacting The Cambridge Crystallographic Data Centre, 12 Union Road, Cambridge CB2 1EZ, UK; fax: + 44 1223 336033.

AUTHOR INFORMATION

Corresponding Author

Antonio M. Echavarren − *Barcelona Institute of Science and Technology, Institute of Chemical Research of Catalonia (ICIQ-CERCA), 43007 Tarragona, Spain; Departament de Química Orgànica i Analítica and Department de Química Física i Inorgànica, Universitat Rovira i Virgili, 43007 Tarragona, Spain;* orcid.org/0000-0001-6808-3007; Email: aechavarren@iciq.es

Authors

Pablo Mora − *Barcelona Institute of Science and Technology, Institute of Chemical Research of Catalonia (ICIQ-CERCA), 43007 Tarragona, Spain; Departament de Química Orgànica i Analítica and Department de Química Física i Inorgànica, Universitat Rovira i Virgili, 43007 Tarragona, Spain*

Imma Escofet − *Barcelona Institute of Science and Technology, Institute of Chemical Research of Catalonia (ICIQ-CERCA), 43007 Tarragona, Spain; Departament de Química Orgànica i Analítica, Universitat Rovira i Virgili, 43007 Tarragona, Spain;* orcid.org/0000-0002-1790-4255

Maria Besora − *Department de Química Física i Inorgànica, Universitat Rovira i Virgili, 43007 Tarragona, Spain;* orcid.org/0000-0002-6656-5827

Federica Cester Bonati − *Barcelona Institute of Science and Technology, Institute of Chemical Research of Catalonia (ICIQ-CERCA), 43007 Tarragona, Spain; Departament de Química Orgànica i Analítica, Universitat Rovira i Virgili, 43007 Tarragona, Spain*

Complete contact information is available at: https://pubs.acs.org/10.1021/acscatal.4c07495

Notes

The authors declare no competing financial interest.

ACKNOWLEDGMENTS

We thank PID2022-136623NB-I00/MICIU/AEI/10.13039/501100011033/FEDER, UE, CEX2019-000925-S/MICIU/AEI/10.13039/501100011033, the European Research Council (Advanced Grant 835080), the AGAUR (2021 SGR 01256), and CERCA Program/Generalitat de Catalunya for financial support. We also thank the ICIQ X-ray diffraction, NMR and mass spectrometry, and chromatography units.

REFERENCES

(1) Noyori, R. Asymmetric Catalysis: Science and Opportunities (Nobel Lecture). *Angew. Chem., Int. Ed.* **2002**, *41*, 2008−2022.
(2) Colacot, T. J. A Concise Update on the Applications of Chiral Ferrocenyl Phosphines in Homogeneous Catalysis Leading to Organic Synthesis. *Chem. Rev.* **2003**, *103*, 3101−3118.
(3) (a) Hayashi, T.; Yamamoto, K.; Kumada, M. Asymmetric Catalytic Hydrosilylation of Ketones Preparation of Chiral Ferrocenylphosphines as Chiral Ligands. *Tetrahedron Lett.* **1974**, *15*, 4405−4408. (b) Hayashi, T.; Mise, T.; Fukushima, M.; Kagotani, M.; Nagashima, N.; Hamada, Y.; Matsumoto, A.; Kawakami, S.; Konishi, M.; Yamamoto, K. Asymmetric synthesis catalyzed by chiral ferrocenylphosphine-transition metal complexes. I. Preparation of chiral ferrocenylphosphines. *Bull. Chem. Soc. Jpn.* **1980**, *53*, 1138−1151.
(4) Blaser, H.-U.; Brieden, W.; Pugin, B.; Spindler, F.; Studer, M.; Togni, A. Solvias Josiphos Ligands: From Discovery to Technical Applications. *Topics in Catalysis.* **2002**, *19*, 3−16.
(5) Togni, A.; Breutel, C.; Schnyder, A.; Spindler, F.; Landert, H.; Tijani, A. A Novel Easily Accessible Chiral Ferrocenyldiphosphine for Highly Enantioselective Hydrogenation, Allylic Alkylation, and Hydroboration Reactions. *J. Am. Chem. Soc.* **1994**, *116*, 4062−4066.
(6) Ireland, T.; Grossheimann, G.; Wieser-Jeunesse, C.; Knochel, P. Ferrocenyl Ligands with Two Phosphanyl Substituents in the α,ε positions for the Transition Metal Catalyzed Asymmetric Hydro-

genation of Functionalized Double Bonds. *Angew. Chem., Int. Ed.* **1999**, *38*, 3212−3215.
(7) Sturm, T.; Weissensteiner, W.; Spindler, F. A Novel Class of Ferrocenyl-Aryl-Based Diphosphine Ligands for Rh- and Ru-Catalysed Enantioselective Hydrogenation. *Adv. Synth. Catal.* **2003**, *345*, 160−164.
(8) Chen, W.; McCormack, P. J.; Mohammed, K.; Mbafor, W.; Roberts, S. M.; Whittall, J. Stereoselective Synthesis of Ferrocene-Based C2-Symmetric Diphosphine Ligands: Application to the Highly Enantioselective Hydrogenation of α-Substituted Cinnamic Acids. *Angew. Chem., Int. Ed.* **2007**, *46*, 4141−4144.
(9) Zhao, Q.; Li, S.; Huang, K.; Wang, R.; Zhang, X. A Novel Chiral Bisphosphine-Thiourea Ligand for Asymmetric Hydrogenation of β,β-Disubstituted Nitroalkenes. *Org. Lett.* **2013**, *15*, 4014−4017.
(10) Ito, Y.; Sawamura, M.; Hayashi, T. Catalytic Asymmetric Aldol Reaction: Reaction of Aldehydes with Isocyanoacetate Catalyzed by a Chiral Ferrocenylphosphine-Gold(I) Complex. *J. Am. Chem. Soc.* **1986**, *108*, 6405−6406.
(11) Wu, Z.; Lebœuf, D.; Retailleau, P.; Gandon, V.; Marinetti, A.; Voituriez, A. Enantioselective Gold(I)-Catalyzed Rearrangement of Cyclopropyl-Substituted 1,6-Enynes into 2-Oxocyclobutyl-Cyclopentanes. *Chem. Commun.* **2017**, *53*, 7026−7029.
(12) Koshikawa, T.; Satoh, M.; Masutomi, K.; Shibata, Y.; Tanaka, K. Gold-Catalyzed Enantioselective Intramolecular Annulation of Ene-Yne-Carbonyls via Benzopyrylium-Type Intermediates. *Eur. J. Org. Chem.* **2019**, *2019*, 1488−1492.
(13) Kim, H.; Choi, S. Y.; Shin, S. Asymmetric Synthesis of Dihydropyranones via Gold(I)-Catalyzed Intermolecular [4 + 2] Annulation of Propiolates and Alkenes. *Angew. Chem., Int. Ed.* **2018**, *57*, 13130−13134.
(14) Urbano, A.; Hernández-Torres, G.; del Hoyo, A. M.; Martínez-Carrión, A.; Carreño, M. C. Mild Access to Planar-Chiral *Ortho*-Condensed Aromatic Ferrocenes via Gold(I)-Catalyzed Cycloisomerization of *Ortho*-Alkynylaryl Ferrocenes. *Chem. Commun.* **2016**, *52*, 6419−6422.
(15) Zi, W.; Toste, F. D. Recent Advances in Enantioselective Gold Catalysis. *Chem. Soc. Rev.* **2016**, *45*, 4567−4589.
(16) Zheng, Y.; Guo, L.; Zi, W. Enantioselective and Regioselective Hydroetherification of Alkynes by Gold-Catalyzed Desymmetrization of Prochiral Phenols with P-Stereogenic Centers. *Org. Lett.* **2018**, *20*, 7039−7043.
(17) Alonso, I.; Trillo, B.; López, F.; Montserrat, S.; Ujaque, G.; Castedo, L.; Lledós, A.; Mascareñas, J. L. Gold-Catalyzed [4C+2C] Cycloadditions of Allenedienes, including an Enantioselective Version with New Phosphoramidite-Based Catalysts: Mechanistic Aspects of the Divergence between [4C+3C] and [4C+2C] Pathways. *J. Am. Chem. Soc.* **2009**, *131*, 13020−13030.
(18) González, A. Z.; Toste, F. D. Gold(I)-Catalyzed Enantioselective [4 + 2]-Cycloaddition of Allene-Dienes. *Org. Lett.* **2010**, *12*, 200−203.
(19) González, A. Z.; Benitez, D.; Tkatchouk, E.; Goddard, W. A.; Toste, F. D. Phosphoramidite Gold(I)-Catalyzed Diastereo- and Enantioselective Synthesis of 3,4-Substituted Pyrrolidines. *J. Am. Chem. Soc.* **2011**, *133*, 5500−5507.
(20) (a) Li, Y.; Li, W.; Zhang, J. Gold-Catalyzed Enantioselective Annulations. *Chem.—Eur. J.* **2017**, *23*, 467−512. (b) Zia, W.; Toste, F. D. Recent advances in enantioselective gold catalysis. *Chem. Soc. Rev.* **2016**, *45*, 4567−4589.
(21) Hamilton, G. L.; Kang, E. J.; Mba, M.; Toste, F. D. A Powerful Chiral Counterion Strategy for Asymmetric Transition Metal Catalysis. *Science* **2007**, *121*, 496−499.
(22) Aikawa, K.; Kojima, M.; Mikami, K. Axial Chirality Control of Gold(biphep) Complexes by Chiral Anions: Application to Asymmetric Catalysis. *Angew. Chem., Int. Ed.* **2009**, *48*, 6073−6077.
(23) Tu, X.-F.; Gong, L.-Z. Highly Enantioselective Transfer Hydrogenation of Quinolines Catalyzed by Gold Phosphates: Achiral Ligand Tuning and Chiral-Anion Control of Stereoselectivity. *Angew. Chem., Int. Ed.* **2012**, *51*, 11346−11349.
(24) Franchino, A.; Martí, À.; Echavarren, A. M. H-Bonded Counterion-Directed Enantioselective Au(I) Catalysis. *J. Am. Chem. Soc.* **2022**, *144*, 3497−3509.
(25) Martí, À.; Montesinos-Magraner, M.; Echavarren, A. M.; Franchino, A. H-Bonded Counterion-Directed Catalysis: Enantioselective Gold(I)-Catalyzed Addition to 2-Alkynyl Enones as a Case Study. *Eur. J. Org. Chem.* **2022**, *2022*, No. e202200518.
(26) Martí, À.; Ogalla, G.; Echavarren, A. M. Hydrogen-Bonded Matched Ion Pair Gold(I) Catalysis. *ACS Catal.* **2023**, *13*, 10217−10223.
(27) Elías-Rodríguez, P.; Benítez, M.; Iglesias-Sigüenza, J.; Díez, E.; Fernández, R.; Lassaletta, J. M.; Monge, D. Hydrogen-Bonding Activation of Gold(I) Chloride Complexes: Enantioselective Synthesis of 3(2H)-Furanones by a Cycloisomerization-Addition Cascade. *Org. Lett.* **2024**, *26*, 5995−6000.
(28) Lin, B.; Xiao, Y.; Yang, T.; Chen, G.-Q.; Zhang, X.; Che, C.-M. Gold-Catalyzed Highly Enantioselective Cycloadditions of 1,6-Enynes and 1,6-Diynes Assisted by Remote Hydrogen Bonding Interaction. *iScience* **2024**, *27*, No. 110876.
(29) (a) Zhang, P.; Wang, Y.; Zhang, Z. M.; Zhang, J. Gold(I)/Xiang-Phos-Catalyzed Asymmetric Intramolecular Cyclopropanation of Indenes and Trisubstituted Alkenes. *Org. Lett.* **2018**, *20*, 7049−7052. (b) Wang, Y.; Zhang, P. C.; Di, X.; Dai, Q.; Zhang, Z. M.; Zhang, J. Gold-Catalyzed Asymmetric Intramolecular Cyclization of *N*-Allenamides for the Synthesis of Chiral Tetrahydrocarbolines *Angew. Chem. Int. Ed.* **2017**, *56*, 15905−15909. (c) Zhang, P. C.; Li, Y. L.; He, J.; Wu, H. H.; Li, Z.; Zhang, L. Simultaneous construction of axial and planar chirality by gold/TY-Phos-catalyzed asymmetric hydroarylation. *Nat. Commun.* **2021**, *12*, 4609. (d) Zhang, Z. M.; Chen, P.; Li, W.; Niu, Y.; Zhao, X. L.; Zhang, L. A New Type of Chiral Sulfinamide Monophosphine Ligands: Stereodivergent Synthesis and Application in Enantioselective Gold(I)-Catalyzed Cycloaddition Reactions. *Angew. Chem., Int. Ed.* **2014**, *53*, 4350−4354.
(30) García-Morales, C.; Ranieri, B.; Escofet, I.; López-Suarez, L.; Obradors, C.; Konovalov, A. I.; Echavarren, A. M. Enantioselective Synthesis of Cyclobutenes by Intermolecular [2 + 2] Cycloaddition with Non-C2 Symmetric Digold Catalysts. *J. Am. Chem. Soc.* **2017**, *139*, 13628−13631.
(31) Wu, Z.; Retailleau, P.; Gandon, V.; Voituriez, A.; Marinetti, A. Use of Planar Chiral Ferrocenylphosphine-Gold(I) Complexes in the Asymmetric Cycloisomerization of 3-Hydroxylated 1,5-Enynes. *Eur. J. Org. Chem.* **2016**, *2016*, 70−75.
(32) Caniparoli, U.; Escofet, I.; Echavarren, A. M. Planar Chiral 1,3-Disubstituted Ferrocenyl Phosphine Gold(I) Catalysts. *ACS Catal.* **2022**, *12*, 3317−3322.
(33) Pérez-Sánchez, J. C.; Herrera, R. P.; Gimeno, M. C. Ferrocenyl Gold Complexes as Efficient Catalysts. *Eur. J. Inorg. Chem.* **2022**, *2022*, No. e202101067.
(34) Zuccarello, G.; Mayans, J. G.; Escofet, I.; Scharnagel, D.; Kirillova, M. S.; Pérez-Jimeno, A. H.; Calleja, P.; Boothe, J. R.; Echavarren, A. M. Enantioselective Folding of Enynes by Gold(I) Catalysts with a Remote *C*2-Chiral Element. *J. Am. Chem. Soc.* **2019**, *141*, 11858−11863.
(35) Zuccarello, G.; Escofet, I.; Caniparoli, U.; Echavarren, A. M. New-Generation Ligand Design for the Gold-Catalyzed Asymmetric Activation of Alkynes. *ChemPlusChem.* **2021**, *86*, 1283−1296.
(36) Zuccarello, G.; Nannini, L. J.; Arroyo-Bondía, A.; Fincias, N.; Arranz, I.; Pérez-Jimeno, A. H.; Peeters, M.; Martín-Torres, I.; Sadurní, A.; García-Vázquez, V.; Wang, Y.; Kirillova, M. S.; Montesinos-Magraner, M.; Caniparoli, U.; Núñez, G. D.; Maseras, F.; Besora, M.; Escofet, I.; Echavarren, A. Enantioselective Catalysis with Pyrrolidinyl Gold(I) Complexes: DFT and NEST Analysis of the Chiral Binding Pocket. *JACS Au* **2023**, *3*, 1742−1754.
(37) Martín-Torres, I.; Ogalla, G.; Yang, J.-M.; Rinaldi, A.; Echavarren, A. M. Enantioselective Alkoxycyclization of 1,6-Enynes with Gold(I)-Cavitands: Total Synthesis of Mafaicheenamine C. *Angew. Chem., Int. Ed.* **2021**, *60*, 9339−9344.
(38) Francos, J.; Grande-Carmona, F.; Faustino, H.; Iglesias-Sigüenza, J.; Díez, E.; Alonso, I.; Fernández, R.; Lassaletta, J. M.;

https://doi.org/10.1021/acscatal.4c07495
ACS Catal. 2025, 15, 2342−2350

López, F.; Mascareñas, J. L. Axially Chiral Triazoloisoquinolin-3-ylidene Ligands in Gold(I)-Catalyzed Asymmetric Intermolecular (4 + 2) Cycloadditions of Allenamides and Dienes. *J. Am. Chem. Soc.* **2012**, *134*, 14322−14325.
(39) Pallova, L.; Abella, L.; Jean, M.; Vanthuyne, N.; Barthes, C.; Vendier, L.; Autschbach, J.; Crassous, J.; Bastin, S.; César, V. Helical Chiral N-Heterocyclic Carbene Ligands in Enantioselective Gold Catalysis. *Chem.−Eur. J.* **2022**, *28*, No. e202200166.
(40) Martinez, T.; Vanitcha, A.; Troufflard, C.; Vanthuyne, N.; Forté, J.; Gontard, G.; Lemière, G.; Mouriès-Mansuy, V.; Fensterbank, L. Indolizy Carbene Ligand. Evaluation of Electronic Properties and Applications in Asymmetric Gold(I) Catalysis. *Angew. Chem.* **2021**, *133*, 20032−20041.
(41) Burckhardt, U.; Hintermann, L.; Schnyder, A.; Togni, A. Synthesis and Structure of Pyrazole-Containing Ferrocenyl Ligands for Asymmetric Catalysis. *Organometallics* **1995**, *14*, 5415−5425.
(42) Togni, A.; Burckhardt, U.; Gramlich, V.; Pregosin, P. S.; Salzmann, R. Palladium-Catalyzed Asymmetric Allylic Amination Using Ferrocenyl Pyrazole Ligands: Steric Control of η3-Allyl Configuration and Site-Selective Nucleophilic Attack. *J. Am. Chem. Soc.* **1996**, *118*, 1031−1037.
(43) Abbas, Z.; Hu, X.-H.; Ali, A.; Xu, Y.-W.; Hu, X.-P. New Chiral Ferrocene/Indole-Based Diphosphine Ligands for Rh-Catalyzed Asymmetric Hydrogenation of Functionalized Olefins. *Tetrahedron Lett.* **2020**, *61*, No. 151860.
(44) Han, M.-L.; Wang, D.-Y.; Zeng, P.-W.; Zheng, Z.; Hu, X.-P. New Chiral Ferrocenyl P,S-Ligands for Highly Diastereo- and Enantioselective Ag(I)-Catalyzed Asymmetric [3 + 2] Cycloaddition of Azomethine Ylides. *Tetrahedron Asymmetry* **2012**, *23*, 306−312.
(45) Marquarding, D.; Klusacek, H.; Gokel, G.; Hoffmann, P.; Ugi, I. Stereoselective Syntheses. VI. Correlation of Central and Planar Chirality in Ferrocene Derivatives. *J. Am. Chem. Soc.* **1970**, *92*, 5389−5393.
(46) Nieto-Oberhuber, C.; López, S.; Echavarren, A. M. Intramolecular [4 + 2] Cycloadditions of 1,3-Enynes or Arylalkynes with Alkenes with Highly Reactive Cationic Phosphine Au(I) Complexes. *J. Am. Chem. Soc.* **2005**, *127*, 6178−6179.
(47) Nieto-Oberhuber, C.; Pérez-Galán, P.; Herrero-Gómez, E.; Lauterbach, T.; Rodríguez, C.; López, S.; Bour, C.; Rosellón, A.; Cárdenas, D. J.; Echavarren, A. M. Gold(I)-Catalyzed Intramolecular [4 + 2] Cycloadditions of Arylalkynes or 1,3-Enynes with Alkenes: Scope and Mechanism. *J. Am. Chem. Soc.* **2008**, *130*, 269−279.
(48) Handa, S.; Slaughter, L. M. Enantioselective Alkynylbenzaldehyde Cyclizations Catalyzed by Chiral Gold(I) Acyclic Diaminocarbene Complexes Containing Weak Au−Arene Interactions. *Angew. Chem., Int. Ed.* **2012**, *51*, 2912−2915.
(49) Herrero-Gómez, E.; Nieto-Oberhuber, C.; López, S.; Benet-Buchholz, J.; Echavarren, A. M. Cationic η1/η2-Gold(I) Complexes of Simple Arenes. *Angew. Chem., Int. Ed.* **2006**, *45*, 5455−5459.
(50) Teller, H.; Flügge, S.; Goddard, R.; Fürstner, A. Enantioselective Gold Catalysis: Opportunities Provided by Monodentate Phosphoramidite Ligands with an Acyclic TADDOL Backbone. *Angew. Chem.* **2010**, *122*, 1993−1997.
(51) See Supporting Information.
(52) Nieto-Oberhuber, C.; Muñoz, M. P.; Buñuel, E.; Nevado, C.; Cárdenas, D. J.; Echavarren, A. M. Cationic Gold(I) Complexes: Highly Alkynophylic Catalysts for the *exo*- and *endo*-Cyclization of Enynes. *Angew. Chem., Int. Ed.* **2004**, *43*, 2402−2406.
(53) Nieto-Oberhuber, C.; Muñoz, M. P.; López, S.; Jiménez-Núñez, E.; Nevado, C.; Herrero-Gómez, E.; Raducan, M.; Echavarren, A. M. Gold(I)-Catalyzed Cyclizations of 1,6-Enynes: Alkoxycyclizations and *exo*/*endo* Skeletal Rearrangements. *Chem.—Eur. J.* **2006**, *12*, 1677−1693.
(54) Escofet, I.; Armengol-Relats, H.; Bruss, H.; Besora, M.; Echavarren, A. M. On the Structure of Intermediates in Enyne Gold(I)-Catalyzed Cyclizations: Formation of *trans*-Fused Bicyclo[5.1.0]octanes as a Case Study. *Chem.—Eur. J.* **2020**, *26*, 15738−15745.
(55) (a) All dataset collection of computational results of this manuscript is available in the ioChem-BD repository and can be accessed through: DOI: 10.19061/iochem-bd-1-362. (b) Álvarez-Moreno, M.; de Graaf, C.; Lopez, N.; Maseras, F.; Poblet, J. M.; Bo, C. Managing the Computational Chemistry Bid Data Problem: The ioChem-BD Platform. *J. Chem. Inf. Model.* **2015**, *55*, 95−103.
(56) (a) Johnson, E. R.; Keinan, S.; Mori-Sánchez, P.; Contreras-García, J.; Cohen, A. J.; Yang, W. Revealing Noncovalent Interactions. *J. Am. Chem. Soc.* **2010**, *132*, 6498−6506. (b) Contreras-García, J.; Johnson, E. R.; Keinan, S.; Chaudret, R.; Piquemal, J. P.; Beratan, D. N.; Yang, W. NCIPLOT: A Program for Plotting Noncovalent Interaction Regions. *J. Chem. Theory Comput.* **2011**, *7*, 625−632.
(57) (a) Seguin, T. J.; Wheeler, S. E. Stacking and Electrostatic Interactions Drive the Stereoselectivity of Silylium-Ion Asymmetric Counteranion-Directed Catalysis. *Angew. Chem., Int. Ed.* **2016**, *55*, 15889−15893. (b) Neel, A. J.; Hilton, M. J.; Sigman, M. S.; Toste, F. D. Exploiting non-covalent π interactions for catalyst design. *Nature* **2017**, *543*, 637−646. (c) Toste, F. D.; Sigman, M. S.; Miller, S. J. Pursuit of Noncovalent Interactions for Strategic Site-Selective Catalysis. *Acc. Chem. Res.* **2017**, *50*, 609−615.
(58) Grimme, S.; Schreiner, P. R. Steric Crowding Can Stabilize a Labile Molecule: Solving the Hexaphenylethane Riddle. *Angew. Chem., Int. Ed.* **2011**, *50*, 12639−12642.
(59) Wagner, J. P.; Schreiner, P. R. Nature Utilized Unusual High London Dispersion Interactions for Compact Membranes Composed of Molecular Ladders. *J. Chem. Theroy Comput.* **2014**, *10*, 1353−1358.
(60) Besora, M.; Olmos, A.; Gava, R.; Noverges, B.; Asensio, G.; Caballero, A.; Maseras, F.; Pérez, P. J. A Quantitative Model for Alkane Nucleophilicity Based on C−H Bond Structural/Topological Descriptors. *Angew. Chem., Int. Ed.* **2020**, *59*, 3112.
(61) *RDKit: Open-source cheminformatics.*, https://www.rdkit.org.

https://doi.org/10.1021/acscatal.4c07495
ACS Catal. 2025, 15, 2342−2350